Electronic Supplementary Material (ESI) for ChemComm.
This journal is © The Royal Society of Chemistry 2021

Supporting Information

Ultrafast Heating to Boost the Electrocatalytic Activity of Iridium towards Oxygen Evolution Reaction

Bohan Deng,[a] Yuanzheng Long ,[a] Cheng Yang,[a] Peng Du,[ab] Ruyue Wang,[ab] Kai Huang[b] and Hui Wu*[a]

[a] State Key Laboratory of New Ceramics and Fine Processing, School of Materials Science and Engineering, Tsinghua University, Beijing, 100084, China. E-mail: huiwu@tsinghua.edu.cn

[b] State Key Laboratory of Information Photonics and Optical Communications & School of Science, Beijing University of Posts and Telecommunications, Beijing 100876, China.

METHODS

Materials Preparation. Carbon paper was purchased from Toray Industries, Inc. The carbon paper was pre-cleaned with ethanol and deionized water for several times and then was treated in a horizontal tube furnace with continuous flow of argon gas at 1173 K for 1 h. After pretreatment, the carbon paper was cut into pieces of 1.0 cm × 4.0 cm and connected to copper foils using copper tapes in order to gain good electrical contact. Iridium trichloride ($IrCl_3$, Sigma-Aldrich) was dissolved in ethanol and 40 μL $IrCl_3$ solution was gradually dropped onto the carbon paper. After the carbon paper was uniformly covered with the Ir precursor solution, a high current pulse (5A, 5s) generated from a DC power (ITECH, IT6502D) was applied to the carbon paper in air. An infrared imaging device (CEM, DT-980H) was used to measure the temperature evolution during the ultrafast heating process. The emissivity ε was set as 0.95 and the reflected temperature compensation (RTC) was set as 298 K. After the heating process, the prepared sample (named as Ir/CP-UH) was cut from copper electrodes and rinsed with ethanol and deionized water for subsequent electrochemical measurements and other characterization.

To compare the effect of ultrafast heating, a contrast sample (named as Ir/CP-NH) was prepared by heating up the carbon paper covered with the Ir precursor solution to 800 K in a muffle furnace with a heating rate of 10 K min^{-1}. Except the heating process, other preparation processes of the Ir/CP-NH were the same as Ir/CP-UH.

Catalyst characterizations. X-ray diffraction analysis was performed by a D/max 2500V diffractometer in reflection mode at 40 kV and 150 mA with a scanning speed of 8 ° min^{-1}. Scanning electron microscopy (SEM) images were taken by a Zeiss microscope (MERLIN VP Compact) operated at 10 kV. HAADF STEM images and HR-TEM images were taken by 2100F transmission electron microscope operated at 200 kV. The Ir loading of the catalysts was confirmed by using an inductively coupled plasma-optical emission spectrometer (Vista-MPX) after sample dissolution. X-ray photoelectron spectra were collected using a Thermo Fisher spectrometer (Escalab 250Xi) equipped with an Al Kα radiation source (1487.6 eV) and hemispherical analyzer with a pass energy of 30.0 eV and energy step size of 0.05 eV. All the XPS spectra were corrected by C 1s peak of 284.8 eV to prevent the charge effect. The raw curves were fitted using XPSPEAK41 software with Shirley backgrounds and Gaussian-Lorentzian functions.

Electrochemical Measurements. All electrochemical tests were carried out on a three-electrode cell connected to an electrochemical workstation (CHI 760E, Shanghai Chenhua Instruments). The alkaline electrolyte and acidic electrolyte were 1.0 M KOH and 0.5 M H_2SO_4 saturated by N_2 respectively. The sample was used as the working electrode (1 cm × 0.5 cm), a graphite rod was used as the counter electrode, and a Hg/HgO electrode and a Ag/AgCl electrode were used as the reference electrode for alkaline electrolyte and acidic electrolyte, respectively. To make a commercial Ir/C catalyst sample, 1mg 20% Ir/C (Premetek) was dispersed into a mixture solution (800 μL of ethanol, 150 μL of ultrapure water and 50 μL of 5wt% Nafion solution). The mixture was treated by ultrasonic for 10 min to make a uniform catalyst ink. Subsequently, 50 μL of catalyst ink was uniformly loaded onto carbon paper (1 cm × 0.5 cm), maintaining the loading of Ir element at 20 μg cm^{-2}. Before electrochemical tests, Cyclic voltammetry (CV) was conducted between 1.0 to 1. 5 V vs. RHE with a scan rates of 100 mV/s for 40 cycles to activate the sample. The OER activity was characterized by linear sweep voltammetry (LSV) over the potential range of 1.2 to 1.7

V vs. RHE at a scan rate of 5 mV/s. To eliminate the effect of solution resistance, the LSV curves were iR corrected by 90% of the solution resistance. The electrochemically active surface area (ECSA) was fitted by cyclic voltammetry curves in the potential of 0−0.1 V vs Hg/HgO at 5−50 mV s^{-1}. Cyclic voltammetry (CV) was conducted between 1.2 V to 1.7 V vs. RHE with a scan rate of 100 mV/s. For stability test, chronopotentiometry was applied at the current of 10 mA/cm^2 for 10h. All assays were run at room temperature.

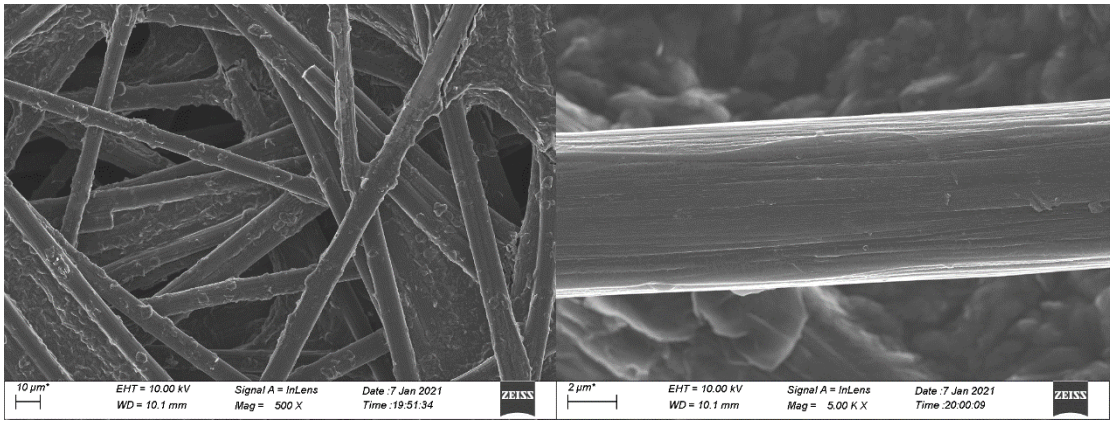

Figure S1. SEM images of original carbon paper at different magnifications.

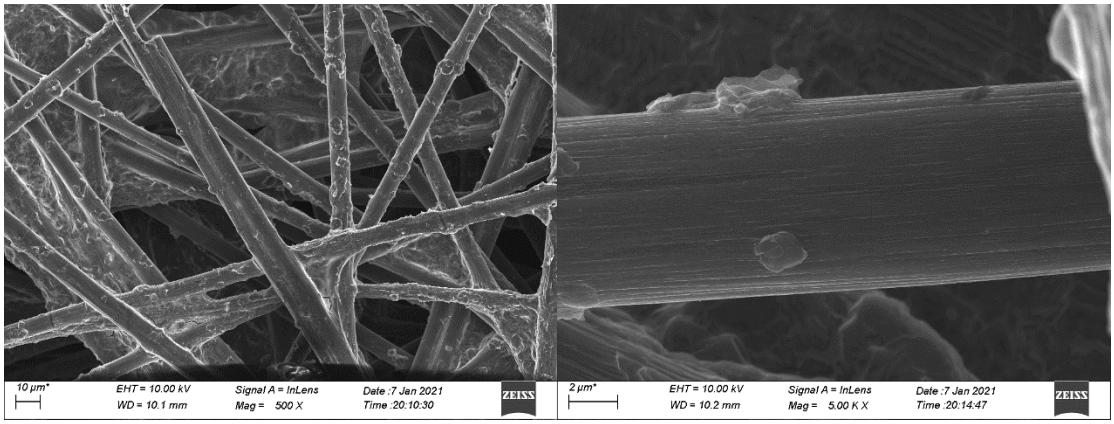

Figure S2. SEM images of Ir/CP-UH at different magnifications.

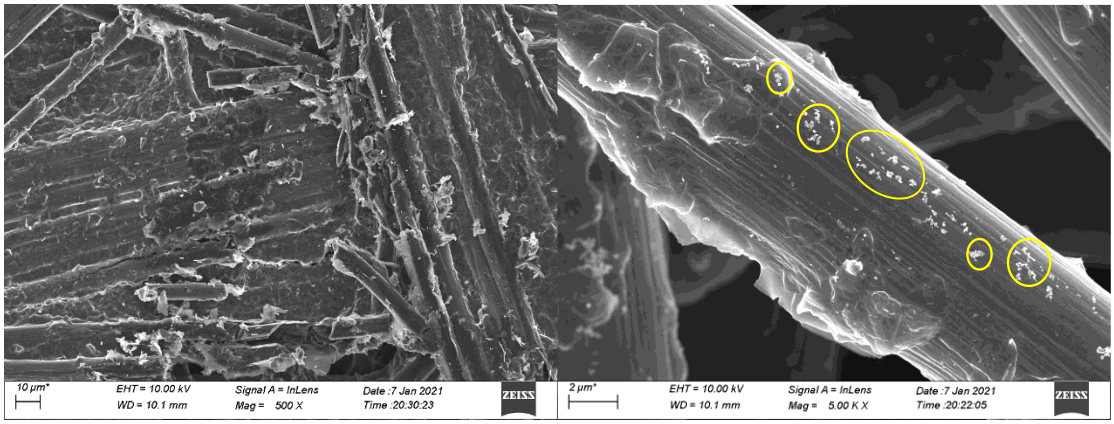

Figure S3. SEM images of Ir/CP-NH at different magnifications. Agglomerate Ir particles with sizes at around 100~300 nm (in yellow circles) can be found in Ir/CP-NH.

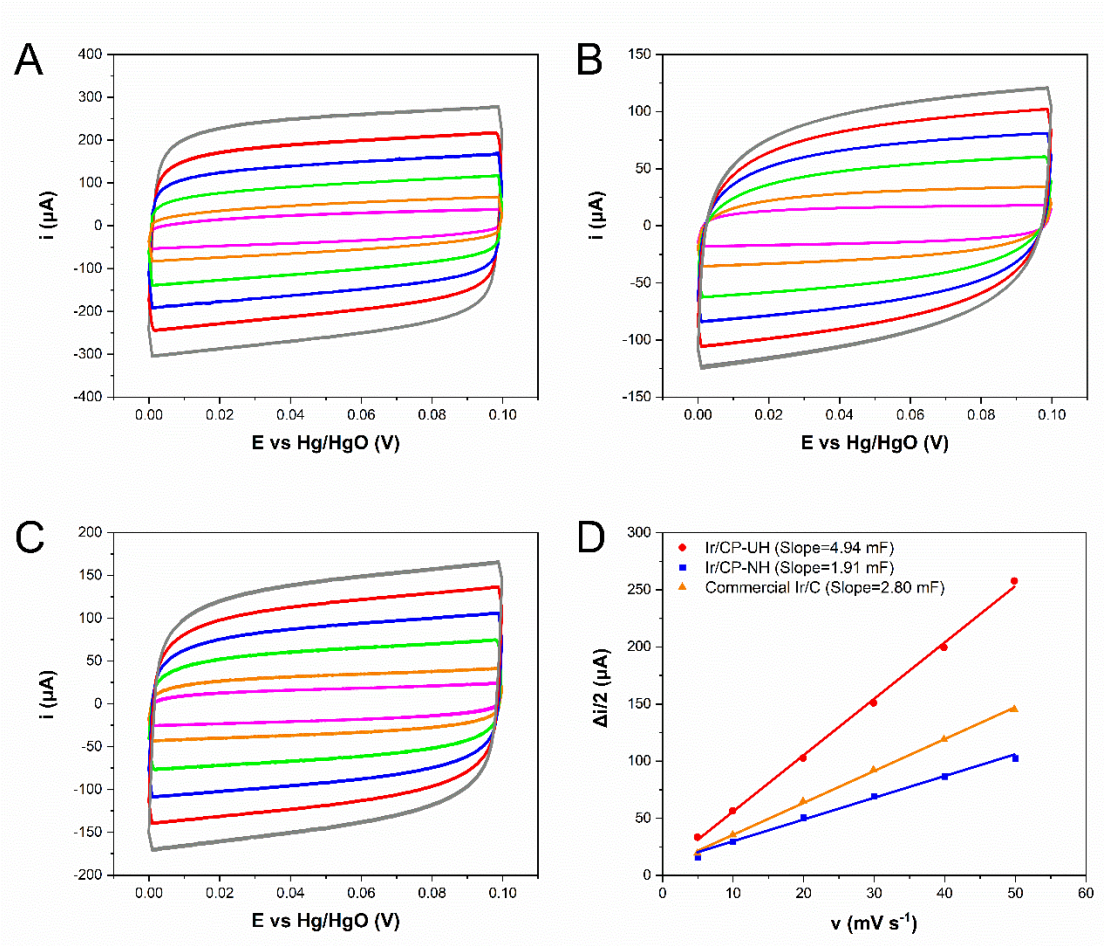

Figure S4. (A-C) CV curves measured in the non-faradaic potential (0-0.1 V vs Hg/HgO) at various scan rates (5, 10, 20, 30, 40 and 50 mV s^{-1}) for (A) Ir/CP-UH, (B) Ir/CP-NH and (C) commercial Ir/C. (D) The half currents difference at 0.05 V vs Hg/HgO plotted as a function of scan rate.

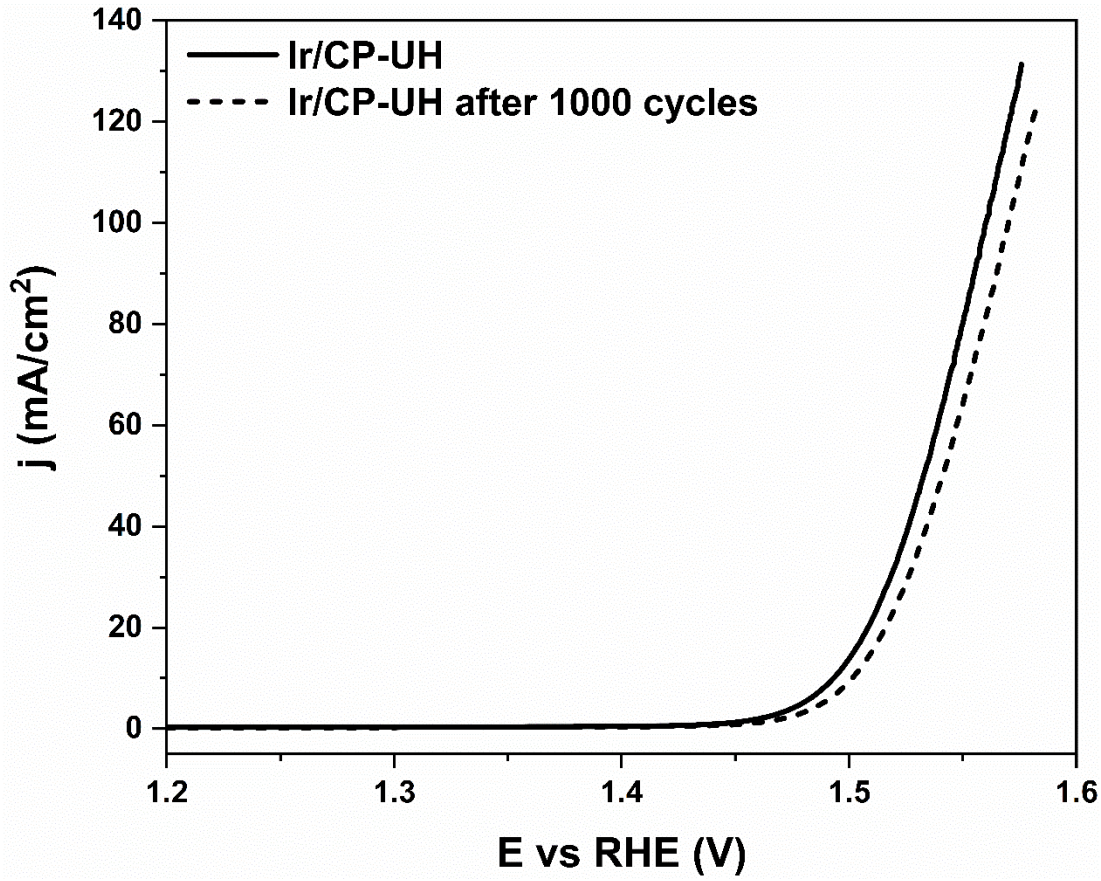

Figure S5. The LSV curves of Ir/CP-UH before and after accelerated CV measurement at 100 mV/s for 1000 cycles.

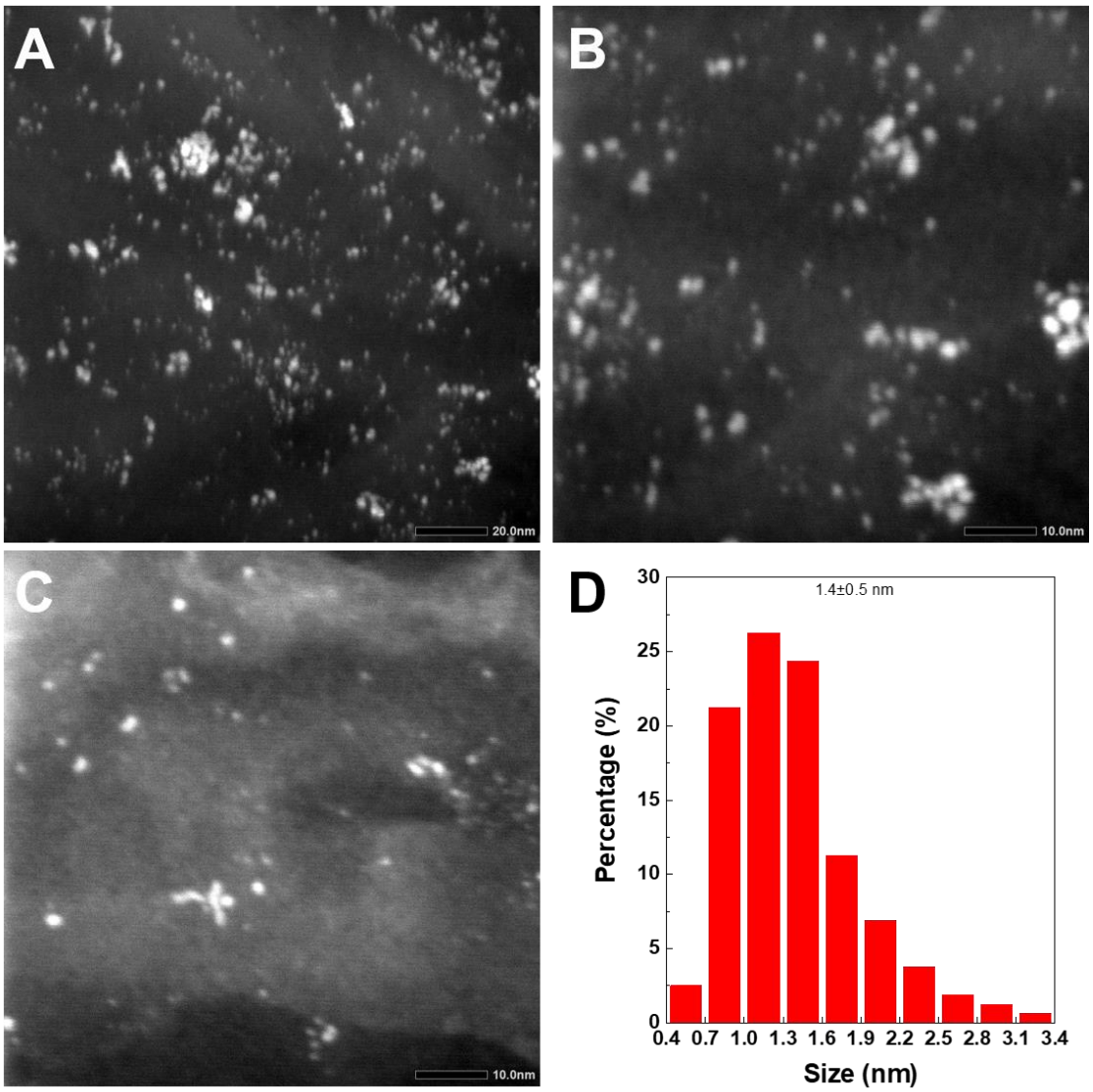

Figure S6. (A-C) STEM images of Ir/CP-UH after stability test (chronopotentiometry at 10 mA cm^{-2}) at different magnifications. (D) Size distribution of Ir in Ir/CP-UH after stability test.

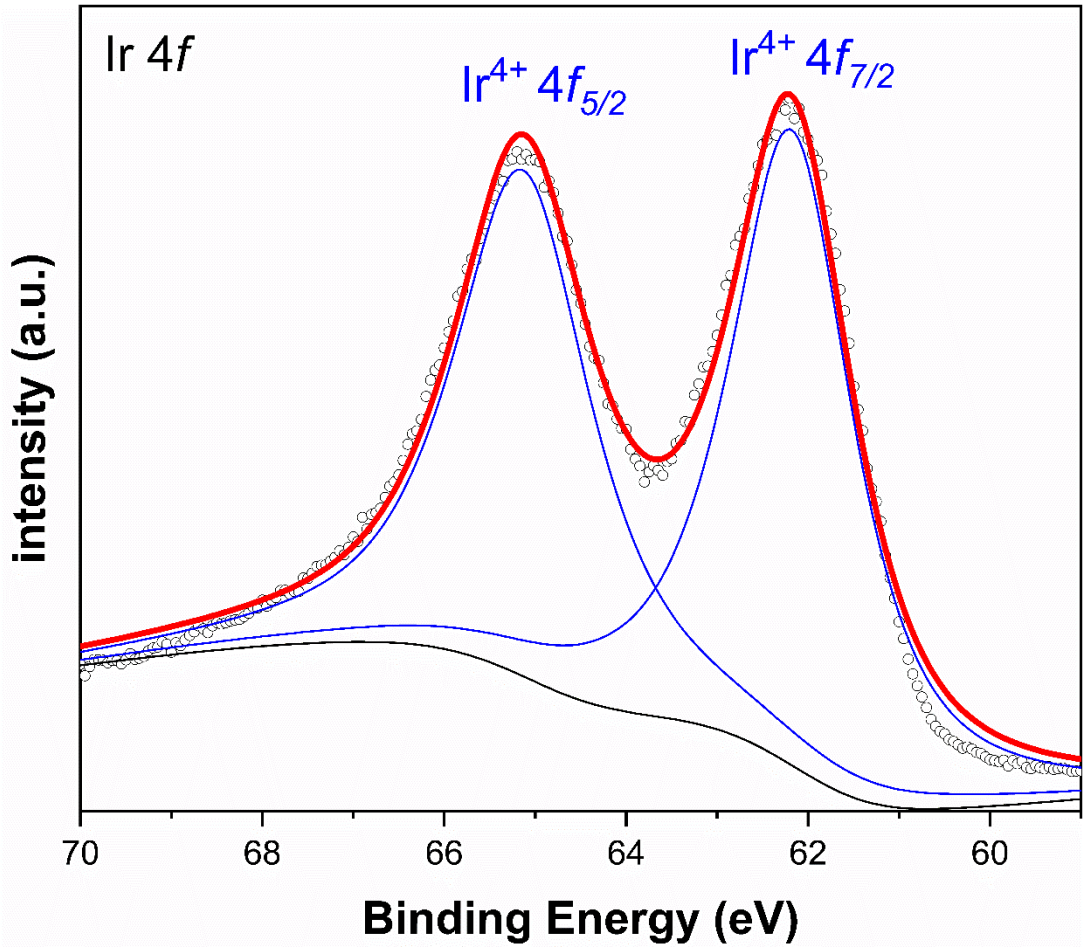

Figure S7. Ir 4*f* XPS spectra of Ir/CP-UH after stability test (chronopotentiometry at 10 mA cm^{-2}). The Ir was oxidized to IrO_2 after OER under high potential, which is the active site for OER.

Table S1. Summary of the OER activity of recently reported Ir based catalysts.

Catalyst	**Electrolyte**	**Ir loading ($\mu g\ cm^{-2}$)**	**Overpotential (mV) at j=10 mA cm^{-2}**	**Tafel slope (mV dec-1)**	**Mass activity ($A\ g_{Ir}^{-1}$) at 1.5V vs RHE**	**Refs.**
Ir/CP-UH	1.0M KOH	12.3	260	41.6	1405	This work
Ir/CP-UH	0.5M H_2SO_4	12.3	264	68.3	981	This work
Co@Ir/NC-10%	1.0M KOH	15.1	280	73.8		[1]
$Ir_{18\ wt\ \%}$-NiO	1.0M KOH	263	215	38		[2]
Ir_1@Co/NC	1.0M KOH	3.6	260	163		[3]
Ir/$Ni(OH)_2$	1.0M KOH	70	224	41		[4]
IrO_x-Ir	0.5M H_2SO_4	133.3	~290	43.7		[5]
Ir/GF	0.5M H_2SO_4	48.5	290	46		[6]
Ir/TiO_2-MoO_x	0.05M H_2SO_4	37.5	290	/		[7]
$IrNiO_x$ /Meso-ATO-180	0.05M H_2SO_4	10.2	~330	/		[8]
IrO_x/$SrIrO_3$	0.5M H_2SO_4	/	270	/		[9]
IrNi-RF	0.1 M $HClO_4$	13.2	313.6	48.6	470 (@1.53V)	[10]
Pt-Ir-Pd nanocages	0.1 M $HClO_4$	16.8 (for Pt+Ir+Pd)	372	128.7	200(@1.53V)	[11]

References

1. D. Li, Z. Zong, Z. Tang, Z. Liu, S. Chen, Y. Tian and X. Wang, Acs Sustainable Chemistry & Engineering, 2018, 6, 5105-5114.
2. Q. Wang, X. Huang, Z. L. Zhao, M. Wang, B. Xiang, J. Li, Z. Feng, H. Xu and M. Gu, J Am Chem Soc, 2020, 142, 7425-7433.
3. W.-H. Lai, L.-F. Zhang, W.-B. Hua, S. Indris, Z.-C. Yan, Z. Hu, B. Zhang, Y. Liu, L. Wang, M. Liu, R. Liu, Y.-X. Wang, J.-Z. Wang, Z. Hu, H.-K. Liu, S.-L. Chou and S.-X. Dou, Angewandte Chemie-International Edition, 2019, 58, 11868-11873.
4. G. Zhao, P. Li, N. Cheng, S. X. Dou and W. Sun, Adv. Mater., 2020, 32.
5. P. Lettenmeier, L. Wang, U. Golla-Schindler, P. Gazdzicki, N. A. Canas, M. Handl, R. Hiesgen, S. S. Hosseiny, A. S. Gago and K. A. Friedrich, Angew Chem Int Ed Engl, 2016, 55, 742-746.
6. J. Zhang, G. Wang, Z. Liao, P. Zhang, F. Wang, X. Zhuang, E. Zschech and X. Feng, Nano Energy, 2017, 40, 27-33.
7. E. J. Kim, J. Shin, J. Bak, S. J. Lee, K. H. Kim, D. Song, J. Roh, Y. Lee, H. Kim, K. S. Lee and E. Cho, Applied Catalysis B-Environmental, 2021, 280.
8. N. Hong Nhan, H.-S. Oh, T. Reier, E. Willinger, M.-G. Willinger, V. Petkov, D. Teschner and P. Strasser, Angewandte Chemie-International Edition, 2015, 54, 2975-2979.
9. L. C. Seitz, C. F. Dickens, K. Nishio, Y. Hikita, J. Montoya, A. Doyle, C. Kirk, A. Vojvodic, H. Y. Hwang, J. K. Norskov and T. F. Jaramillo, Science, 2016, 353, 1011-1014.
10. H. Jin, Y. Hong, J. Yoon, A. Oh, N. K. Chaudhari, H. Baik, S. H. Joo and K. Lee, Nano Energy, 2017, 42, 17-25.
11. J. W. Zhu, M. H. Xie, Z. T. Chen, Z. H. Lyu, M. F. Chi, W. Q. Jin and Y. N. Xia, Advanced Energy Materials, 2020, 10.